# Generation of nonreciprocity in gapless spin waves by chirality injection

Gyungchoon Go, Seunghun Lee, and Se Kwon Kim [*]

*Department of Physics, Korea Advanced Institute of Science and Technology, Daejeon 34141, Korea*

It is known that in chiral magnets with intrinsic inversion symmetry breaking, two spin waves moving in opposite directions can propagate at different velocities, exhibiting a phenomenon called magnetochiral nonreciprocity, which allows for realizations of certain spin logic devices such as a spin-wave diode. Here, we theoretically demonstrate that the spin-wave nonreciprocity can occur without intrinsic bulk chirality in easy-cone ferromagnets and easy-cone antiferromagnets. Specifically, we show that nonlocal injection of a spin current from proximate normal metals to easy-cone magnets engenders a nonequilibrium chiral spin texture, on top of which spin waves exhibit nonreciprocity proportional to the injected spin current. In particular, the easy-cone ferromagnet is shown to support the spin-wave nonreciprocity without an external field, in contrast to the previously known easy-plane ferromagnetic counterpart that requires an external field, thereby providing a field-free means to manipulate the spin-wave nonreciprocity. One notable feature of the nonreciprocal spin waves is their gapless nature, which can lead to a large thermal rectification effect at sufficiently low temperatures.

## I. INTRODUCTION

It is known that in certain materials with broken inversion symmetry, direction-dependent propagation of particles can occur [1]. In particular, chiral magnetic materials, in which both the inversion symmetry and the time-reversal symmetry are broken, are known to harbor such a nonreciprocal transport of spin waves [2,3]. Because spin waves carry energy and angular momentum without accompanying the Joule heating, the nonreciprocal spin-wave phenomenon can be exploited to realize energy-efficient spin devices such as spin-wave logic gates [4] and spin-wave diodes [5]. The nonreciprocal propagation of spin waves is attributed to the asymmetric dispersion $\omega(k) \neq \omega(-k)$, which, for long-wavelength modes, can often be written as

$$\omega(k) = \omega_0(k) + Ck, \qquad (1)$$

where $\omega_0(k)$ represents the symmetric component and the $k$-linear term is responsible for the spin-wave nonreciprocity. The latter has been interpreted as the spin-wave Doppler shift that can be induced by the spin-polarized current [6–9], the magnetostatic interactions [10], the Dzyaloshinskii-Moriya interaction [11–20], and the phonon and magnon drags [21,22]. We note that the aforementioned nonreciprocal spin waves possess a finite energy gap.

Recently, it was recognized that it is possible to electrically inject chirality into nonchiral magnetic materials with easy-plane or easy-cone anisotropy, whose order parameter is characterized by a U(1) azimuthal angle which we denote by $\phi$, in the context of superfluid spin transport [23–29]. Experimental schemes for superfluid spin transport have been proposed by using the nonlocal spin injection from proximate normal metals via the spin Hall effect [30,31]; their

realizations have been reported for $Cr_2O_3$ [32] and quantum-Hall graphene [33]. In superfluid spin transport, the spin supercurrent is proportional to the gradient of the U(1) parameter $\phi'$, which manifests as a chiral spin texture [23]. Long-wavelength spin waves in easy-plane and easy-cone magnets in equilibrium have a symmetric linear dispersion: $\omega(k) = c|k|$, which is gapless since it is the Goldstone mode associated with spontaneous breaking of the U(1) symmetry.
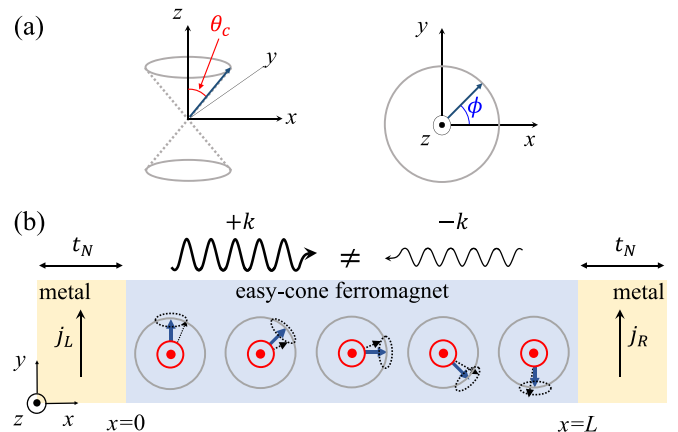


FIG. 1. (a) Schematic illustrations of ground states of easy-cone ferromagnets. The ground state manifolds are shown as solid gray lines, which form two cones with the cone angle $\theta_c$ from the $z$ axis. The azimuthal angle $\phi$ is arbitrarily chosen in a ground state, breaking the U(1) spin-rotational symmetry spontaneously. (b) Geometrical setup of the circuit configuration for the spin current injection. The spin configuration is shown for the symmetric case where the left and right currents are identical ($j_L = j_R$). The chiral spin texture ($z$ component: red circled dots; $xy$ component: solid blue arrows) is induced by nonlocal spin injection from the two boundaries. The spin waves on top of the chiral spin texture (dotted black arrows) show a direction-dependent propagation characterized by the group-velocity difference between $+k$ and $-k$ (wavy arrows).

*sekwonkim@kaist.ac.kr

The ability to maintain a chiral spin texture in easy-plane and easy-cone magnets through a nonlocal spin injection leads us to wonder whether the injected chirality can induce nonreciprocity in an otherwise reciprocal gapless spin-wave spectrum.

Indeed, it was shown that the spin-wave nonreciprocity can be induced by a spin-current injection in easy-plane ferromagnets subjected to an external field [34–38] as well as in easy-plane antiferromagnets [38]. However, the necessity of an external field is detrimental for scaling spintronics devices [39–43]. Therefore, for practical applications, the ability to generate nonreciprocal spin waves without an external field, for which we consider easy-cone magnets in this work, is highly desired.

In this paper, we theoretically investigate spin waves in easy-cone magnets subjected to a nonlocal injection of the spin current. See Fig. 1 for an illustration of the system. First, we show that the chiral spin texture induced by the spin-current injection leads to the asymmetric dispersion of gapless spin waves in an easy-cone ferromagnet in the absence of an external field, which is in contrast to the easy-plane ferromagnetic case, where the external field is required [34–38]. The induced spin-wave nonreciprocity is proportional to the spin supercurrent $\propto \phi'$ carried by the chiral spin texture, which is analogous to the Doppler shift of the Bogoliubov quasiparticle by the superfluid velocity in superfluids [44]. We then expand our result to easy-cone antiferromagnets, which harbor two spin-wave modes, one gapless and the other gapful, unlike the ferromagnetic case, which possesses only a gapless mode. We show that the dispersions of both spin-wave modes become nonreciprocal in the presence of a chiral spin texture when a magnetic field is applied along the high-symmetry axis. For both ferromagnets and antiferromagnets, nonreciprocal spin waves are shown to give rise to nonreciprocal thermal transport within the Boltzmann transport theory. The obtained nonreciprocal spin waves are characterized by two features. First, the nonreciprocity in spin waves is induced nonlocally in nonchiral magnets by the injection of the spin current through the boundaries. Second, the obtained nonreciprocal spin waves are gapless, which can lead to a stronger thermal rectification effect at sufficiently low temperatures compared to gapped counterparts. Our results show that the nonlocal induction of chirality via interfacial spin-current injection can engender magnetochiral phenomena in easy-cone magnetic materials with no intrinsic chirality and with no external field under certain conditions, which can be exploited to realize strongly nonreciprocal thermal transport.

## II. SPIN-WAVE DYNAMICS IN EASY-CONE FERROMAGNETS

We begin by considering the following Hamiltonian density for a quasi-one-dimensional uniaxial ferromagnet:

$$\mathcal{H} = \frac{A}{2}[\nabla \mathbf{n}(x)]^2 - \frac{K_1}{2}n_z(x)^2 + \frac{K_2}{2}n_z(x)^4, \quad (2)$$

where $\mathbf{n}(x) = \mathbf{s}(x)/s$ is a unit vector along the local spin density $\mathbf{s}(x)$, $A$ is the exchange coefficient, $K_1$ is the first-order effective anisotropy, and $K_2$ is the second-order anisotropy. It is convenient to parametrize $\mathbf{n}$ in the spherical coordinates:

$\mathbf{n} = (\sin\theta\cos\phi, \sin\theta\sin\phi, \cos\theta)$. Depending on the relative magnitude of $K_1$ and $K_2$, an equilibrium state is chosen among perpendicular magnetic anisotropy ($\mathbf{n}_0 = \pm\hat{\mathbf{z}}$), in-plane magnetic anisotropy ($\mathbf{n}_0 \perp \hat{\mathbf{z}}$), and easy-cone magnetic anisotropy [see Fig. 1(a)]. In this work, we are interested in easy-cone phases, which are stabilized for $K_1 > 0$ and $K_2 > K_1/2$ [45]. Exemplary materials for easy-cone phases are Co/Pt multilayers, Ta/CoFeB/MgO, and NdFeB compounds [46–49]. The ground-state manifolds are two cones characterized by polar angles (referred to as cone angles): $\theta_c = [\cos^{-1}(K_1 - K_2)/K_2]/2$ and $\pi - \theta_c$. The Hamiltonian [Eq. (2)] is invariant under the azimuthal-angle translation $\phi \to \phi + \Delta\phi$, possessing U(1) spin-rotational symmetry [28]. A ground state breaks the U(1) symmetry, which enables superfluid spin transport [23], as the spontaneous breaking of the U(1) phase symmetry allows for superfluid mass transport in superfluid helium.

Now, let us consider the setup shown in Fig. 1(b), where two heavy metals sandwich the easy-cone ferromagnet. The charge currents through the heavy metals inject a spin current into the magnet via the spin Hall effect. Throughout this paper, we consider situations where the two charge currents are the same ($j_L = j_R = j$), so that the realization of a static spin texture is allowed by the symmetry [31]. The dynamics is described by the Landau-Lifshitz-Gilbert (LLG) equation:

$$s\dot{\mathbf{n}} + \alpha s\mathbf{n} \times \dot{\mathbf{n}} = \mathbf{n} \times \left(A\mathbf{n}'' + K_1 n_z\hat{\mathbf{z}} - 2K_2 n_z^3\hat{\mathbf{z}}\right), \quad (3)$$

where $s$ is the spin density, $\alpha$ is the Gilbert damping constant, and $''$ represents the second-order derivative with respect to $x$. The boundary conditions are given by equating the spin current $J_z = -A\hat{\mathbf{z}} \cdot (\mathbf{n} \times \mathbf{n}')$ with the spin torque subtracted from the spin pumping:

$$-A\sin^2\theta\phi' = \sin^2\theta(j\vartheta \mp \gamma\dot{\phi}), \quad (4)$$

where the upper and the lower signs correspond to the left ($x = 0$) and right ($x = L$) interfaces, respectively [31,50]. Here, $\vartheta$ is related to the effective interfacial spin Hall angle $\theta$ via $\vartheta \equiv \hbar\tan\theta/2et_N$ ($e$ is the charge of an electron, $t_N$ is the normal metal thickness), $\gamma = \hbar g^{\uparrow\downarrow}/4\pi$, and $g^{\uparrow\downarrow}$ is the effective interfacial spin-mixing conductance. By solving the LLG equation in conjunction with the boundary conditions, one can show that the spin-current injection from the boundaries induces a static chiral spin texture characterized by the uniform spatial rotation of the azimuthal angle $\phi \to \phi_0 + \phi'x$, with $\phi' = -\vartheta j/A$, and a cone-angle deformation $\theta_c \to \{\cos^{-1}[K_1 - K_2 + A(\phi')^2]/K_2\}/2$ (see Appendixes A and B for the calculation details of the steady-state solution for chiral spin textures and the spin waves on top of it). Here, note that the spin chirality $\phi' \propto j$ can be dynamically controlled by varying the charge current $j$ in heavy metals.

To investigate spin waves on top of the static spin texture, we divide $\mathbf{n}(x, t)$ into the static profile $\mathbf{n}_0(x)$ and small fluctuations $\delta\mathbf{n}(x, t)$, the latter of which can be written as $\delta\mathbf{n} = n_\theta\hat{\boldsymbol{\theta}} + n_\phi\hat{\boldsymbol{\phi}}$, where $\hat{\boldsymbol{\theta}} = [\partial_\theta\mathbf{n}]|_{\mathbf{n}_0}$ and $\hat{\boldsymbol{\phi}} = \mathbf{n}_0 \times \hat{\boldsymbol{\theta}}$. By expanding the LLG equation to linear order in $n_\theta$ and $n_\phi$ with $\alpha = 0$, we obtain the equations of motion for spin waves:

$$s\dot{n}_\theta = -An_\phi'' - 2An_z^{\text{eq}}\phi'n_\theta',$$
$$s\dot{n}_\phi = An_\theta'' - K_{\phi'}n_\theta - 2An_z^{\text{eq}}\phi'n_\phi', \quad (5)$$
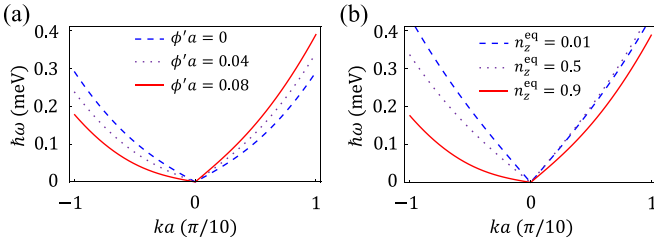
FIG. 2. Spin-wave dispersions [Eq. (6)] (a) for several spin chiralities $\phi'$ with fixed $n_z^{\mathrm{eq}} = 0.9$ and (b) for several values of $n_z^{\mathrm{eq}}$ with fixed $\phi'a = 0.08$, where $a$ is the lattice constant. The asymmetry of the band between $k > 0$ and $k < 0$ increases as $\phi'$ and $n_z^{\mathrm{eq}}$ increase.

where $n_z^{\mathrm{eq}} = \cos\theta_c$, $K_{\phi'} = \bar{K}_1(2K_2 - \bar{K}_1)/K_2$, and $\bar{K}_1 = K_1 + A(\phi')^2$ is a renormalized first-order anisotropy. We note that the last terms in Eqs. (5) are proportional to the product of $n_z^{\mathrm{eq}}$ and the spin-chirality parameter $\phi'$, which give rise to the spin-wave nonreciprocity, as shown below. Inserting a plane-wave ansatz $n_\theta, n_\phi \propto e^{i(kx - \omega t)}$ into Eqs. (5) yields the following spin-wave dispersion:

$$\omega(k) = \frac{1}{s}\sqrt{Ak^2[Ak^2 + K_{\phi'}]} + \frac{2A}{s}n_z^{\mathrm{eq}}\phi'k. \tag{6}$$

When $\phi' = 0$, the first term in Eq. (6) describes a reciprocal spin-wave mode without the spin-current injection: $\omega \approx v_0|k|$, where $v_0 = \sqrt{AK_0}/s$ for sufficiently small $k$. It is the second term that creates the difference between right-moving spin waves ($k > 0$) and left-moving spin waves ($k < 0$), which propagate at velocities $v_+ = v_0 + \delta v$ and $v_- = v_0 - \delta v$, respectively, with $\delta v = (2An_z^{\mathrm{eq}}\phi')/s$ for sufficiently small $k$. Note that the velocity difference is proportional to the spin chirality $\phi'$, which was originally injected nonlocally from proximate metals via spin-current injection. This is our first main result: the injection of the spin current into easy-cone ferromagnets gives rise to the nonreciprocity in otherwise reciprocal spin waves in the absence of an external field, which differs from the previously known easy-plane ferromagnetic case, where an external field is indispensable [34–38]. The spin-wave nonreciprocity increases as $\phi'$ and $n_z^{\mathrm{eq}}$ increase, although there is an upper limit on the induced chirality $\phi'$ for the stability of the spin texture (Landau criterion) [23,24,51–54]. In our case, the maximum value of $\phi'$ for the stable spin wave is given by $\phi'_{\max} = \sqrt{(2K_2 - K_1)/(3A)}$. To confirm our continuum theory for the spin-wave nonreciprocity by using the discrete spin model, we provide its Holstein-Primakoff magnon description in Appendix C.

To plot the spin-wave dispersion numerically, we adopt material parameters of yttrium iron garnet films: $A = 3.7 \times 10^{-7}$ erg/cm [55], $a = 1.23$ nm, and $s/\hbar = 0.65 \times 10^{22}$ cm$^{-3}$ [56], where $a$ and $s$ are a lattice constant and spin angular momentum density, respectively. By using a spin Hall angle of a $\beta$-W thin film ($\theta = 0.3$) [57], we estimate $\phi' \approx 0.08/a$ for $j = 2.4 \times 10^8$ A/cm$^2$. For the effective magnetic anisotropy, we use $K_1 = 2.9 \times 10^6$ erg/cm$^3$ [56,58–60]. The second-order anisotropy constant is chosen to be $K_2 > K_1/2$. Figures 2(a) and 2(b) show the spin-wave dispersion for different spin-chirality parameters $\phi'$ and out-of-plane spin components $n_z^{\mathrm{eq}}$.

## III. SPIN-WAVE DYNAMICS IN EASY-CONE ANTIFERROMAGNETS

Let us now investigate an analogous phenomenon in easy-cone antiferromagnets. We consider a quasi-one-dimensional uniaxial bipartite antiferromagnet which can be described by the following Lagrangian density:

$$\mathcal{L} = s\mathbf{m}\cdot(\mathbf{n}\times\dot{\mathbf{n}}) - \frac{A}{2}(\partial_i\mathbf{n})^2$$
$$- \frac{\mathbf{m}^2}{2\chi} + \frac{K_1}{2}n_z^2 - \frac{K_2}{2}n_z^4 - \mathbf{b}\cdot\mathbf{m}, \tag{7}$$

where $\mathbf{n} = (\mathbf{m}_1 - \mathbf{m}_2)/2$ and $\mathbf{m} = \mathbf{m}_1 + \mathbf{m}_2$ are, respectively, the staggered (Néel) order parameter and the uniform component of the two sublattice spin directions $\mathbf{m}_1$ and $\mathbf{m}_2$ [30,61], $s$ is the saturated spin density, $A$ is the exchange coefficient, $\chi$ is the spin susceptibility, $K_1(> 0)$ and $K_2(> K_1/2)$ are the first- and second-order anisotropy coefficients, respectively, and $\mathbf{b}$ represents the external magnetic field. The equations of motion for $\mathbf{n}$ and $\mathbf{m}$ are obtained by minimizing the action with constraints $|\mathbf{n}| = 1$ and $\mathbf{n}\cdot\mathbf{m} = 0$:

$$s\dot{\mathbf{n}} = \frac{1}{\chi}(\mathbf{m}\times\mathbf{n}) + \mathbf{b}\times\mathbf{n}, \tag{8}$$

$$s\dot{\mathbf{m}} = \mathbf{n}\times\left[A\nabla^2\mathbf{n} + (K_1n_z - 2K_2n_z^3)\hat{\mathbf{z}}\right] + \mathbf{b}\times\mathbf{m}. \tag{9}$$

In terms of the spherical coordinate fields, we write $\mathbf{n} = (\sin\theta\cos\phi, \sin\theta\sin\phi, \cos\theta)$ and $\mathbf{m} = m_\theta\hat{\boldsymbol{\theta}} + m_\phi\hat{\boldsymbol{\phi}}$. In a way similar to the ferromagnetic case, we read a quasiequilibrium solution when the two charge currents in the adjacent heavy metals are the same ($j_L = j_R = j$) [31]:

$$\phi' = -\frac{\vartheta j}{A}, \quad \theta_c = \frac{1}{2}\cos^{-1}\left(\frac{\bar{K}_1 - K_2 - b_0^2\chi}{K_2}\right),$$

$$m_\phi = 0, \quad m_\theta = -\chi b_0\sin\theta_c, \tag{10}$$

where $b_0$ is the magnitude of the perpendicular magnetic field ($\mathbf{b} = -b_0\hat{\mathbf{z}}$) and $\bar{K}_1 = K_1 + A(\phi')^2$. To obtain the spin-wave solution, we consider small deviations $\psi(x, t) = (\delta\theta, \xi_\phi, \delta\phi, \xi_\theta)$ from the equilibrium state defined by

$$\phi \to \phi'x + \frac{\delta\phi}{\sin\theta_c}, \quad \theta \to \theta_c + \delta\theta,$$

$$m_\phi \to \xi_\phi, \quad m_\theta \to -\chi b_0\sin\theta_c + \xi_\theta. \tag{11}$$

Then, the linearized equations of motion for $\psi \propto \exp(ikx - i\omega t)$ yield the eigenvalue problem $(s\omega)\psi = \hat{h}\psi$ with

$$\hat{h} = i\begin{pmatrix} 0 & \chi^{-1} & 0 & 0 \\ -Ak^2 - \kappa_{\phi'} & 0 & -2ikAn_z^{\mathrm{eq}}\phi' & -2b_0n_z^{\mathrm{eq}} \\ -b_0n_z^{\mathrm{eq}} & 0 & 0 & -\chi^{-1} \\ -2ikAn_z^{\mathrm{eq}}\phi' & b_0n_z^{\mathrm{eq}} & Ak^2 & 0 \end{pmatrix}, \tag{12}$$

where $\kappa_{\phi'} = (\bar{K}_1 - \chi b_0^2)[2(K_2 + \chi b_0^2) - \bar{K}_1]/K_2$. When the staggered order parameter lies on the film plane ($n_z^{\mathrm{eq}} = 0$), the effective Hamiltonian [Eq. (12)] is divided by two block-diagonal matrices for two basis functions, $\psi_1 = (\delta\theta, \xi_\phi)$ and $\psi_2 = (\delta\phi, \xi_\theta)$, which have eigenvalues $\epsilon_1(k) = \sqrt{[Ak^2 + \kappa_{\phi'}]/\chi}$ and $\epsilon_2(k) = \sqrt{Ak^2/\chi}$, respectively [30]. The former and the latter describe the gapful spin wave and the
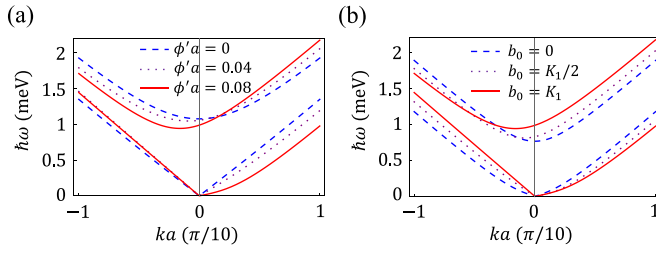
FIG. 3. Spin-wave dispersion of easy-cone antiferromagnets obtained from Eq. (12) (a) for several spin chiralities $\phi'$ and (b) for several magnetic fields $b_0$. Both gapless and gapful spin waves exhibit nonreciprocity. For (a), $K_2 = 1.71 \times 10^6$ erg/cm³ and $b_0 = K_1$ are used. For (b), $K_2 = 1.71 \times 10^6$ and $\phi'a = 0.1$ are used.

gapless spin wave, respectively, of easy-plane antiferromagnets. By turning on $\phi'$ and $n_z^{eq}$, these basis functions hybridize, and the eigenvalues are disturbed. In our model, the spin-wave nonreciprocity is generated when $\phi'$, $n_z^{eq}$, and $b_0$ are all finite, as discussed below.

To obtain the spin-wave dispersion numerically, we adopt the same parameters as in the easy-cone ferromagnet case: $A = 3.7 \times 10^{-7}$ erg/cm, $a = 1.23$ nm, $s/\hbar = 0.65 \times 10^{22}$ cm³, $\theta = 0.3$, and $K_1 = 2.9 \times 10^6$ erg/cm³. In Figs. 3(a) and 3(b), we show the spin-wave dispersion for different spin chiralities $\phi'$ and magnetic fields $b_0$ when $n_z^{eq}$ is finite. When $\phi'$, $b_0$, and $n_z^{eq}$ are all finite, both the upper and lower bands are asymmetric, and the spin-wave nonreciprocity increases with $\phi'$ and $b_0$. This is our second main result: the nonlocal spin-current injection into an easy-cone antiferromagnet generates the nonreciprocity in both gapless and gapful spin waves when the magnet is subjected to an external field.

## IV. THERMAL RECTIFICATION

The asymmetric spin-wave dispersion can give rise to the nonreciprocal heat transport, i.e., thermal rectification, as a nonlinear effect of the temperature gradient [62,63]. Within the framework of the Boltzmann transport, the thermal conductivities are obtained for nonreciprocal spin waves in easy-cone ferromagnets and easy-cone antiferromagnets. Although the two-fluid description [38,64] can be invoked for the complete characterization of thermal transport, we consider heat transport only by thermal magnons. To this end, we consider the Boltzmann transport equation in the relaxation time approximation

$$\frac{\partial g}{\partial t} + v\frac{\partial g}{\partial x} + \dot{k}\frac{\partial g}{\partial k} = -\frac{g - g_0}{\tau}, \tag{13}$$

where $\tau$ is the relaxation time and $g$ and $g_0(\epsilon, T) = (e^{\epsilon/k_B T} - 1)^{-1}$ are nonequilibrium and equilibrium distribution functions, respectively. Because we are interested in a stationary $g$ (i.e., $\partial_t g = 0$) when only the temperature gradient is given for the sample, the Boltzmann equation reduces to

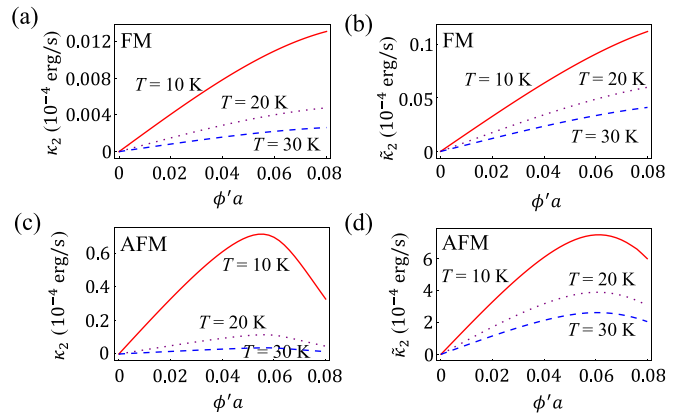$$v\frac{\partial g}{\partial x} = -\frac{g - g_0}{\tau}. \tag{14}$$



FIG. 4. The second-order thermal conductivities [Eq. (18)] as a function of the chirality $\phi'a$. (a) and (b) show the second-order thermal conductivities $\kappa_2$ and $\tilde{\kappa}_2$ in the ferromagnetic model, respectively. (c) and (d) show the second-order thermal conductivities $\kappa_2$ and $\tilde{\kappa}_2$ in the antiferromagnetic model, respectively.

Up to second order in the derivatives of the temperature $T$, the nonequilibrium distribution function can be written as

$$g(\epsilon, T, \partial_x T, \partial_x^2 T) = g_0(\epsilon, T) + g_1(\epsilon, \partial_x T)$$
$$+ g_2(\epsilon, (\partial_x T)^2) + \tilde{g}_2(\epsilon, \partial_x^2 T). \tag{15}$$

By substituting the distribution function (15) into the Boltzmann equation (14), we obtain

$$g_1 = -v\tau\frac{\partial g_0}{\partial T}\frac{\partial T}{\partial x},$$
$$g_2 = v^2\tau^2\frac{\partial^2 g_0}{\partial T^2}\left(\frac{\partial T}{\partial x}\right)^2,$$
$$\tilde{g}_2 = v^2\tau^2\frac{\partial g_0}{\partial T}\frac{\partial^2 T}{\partial x^2}. \tag{16}$$

The heat flux through the sample is

$$j^{heat} = \int dk\,\epsilon(k)v(k)g(\epsilon, T, \partial_x T, \partial_x^2 T), \tag{17}$$

where the $k$ integral is over the first Brillouin zone. Substituting Eqs. (16) into Eq. (17), we have $j^{heat} = -\kappa_1(\partial_x T/T) + \kappa_2(\partial_x T/T)^2 + \tilde{\kappa}_2(\partial_x^2 T/T)$, where

$$\kappa_1 = \int dk\,\epsilon(k)v(k)^2\tau\left(T\frac{\partial g_0}{\partial T}\right),$$
$$\kappa_2 = \int dk\,\epsilon(k)v(k)^3\tau^2\left(T^2\frac{\partial^2 g_0}{\partial T^2}\right), \tag{18}$$
$$\tilde{\kappa}_2 = \int dk\,\epsilon(k)v(k)^3\tau^2\left(T\frac{\partial g_0}{\partial T}\right).$$

Here, $\kappa_2$ and $\tilde{\kappa}_2$ are the second-order thermal conductivities that result in the thermal rectification. For a quantitative estimation, we use the following parameters: sample length $L = 1$ $\mu$m, the temperature difference across the sample $\delta T/T = 10^{-2}$, and the spin-wave relaxation time $1/\tau = 10^5$ s$^{-1}$ [65]. In Fig. 4, we show the second-order thermal conductivities ($\kappa_2$ and $\tilde{\kappa}_2$) as functions of the spin chirality. The second-order
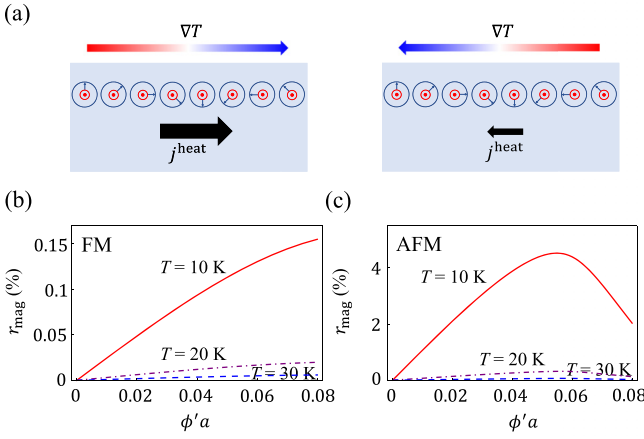
FIG. 5. (a) Schematic illustration of the nonreciprocal thermal transport. The thermal rectification ratio of the magnons $r_{mag}$ [Eq. (19)] (b) in the ferromagnetic model (FM) and (c) in the antiferromagnetic model (AFM). For (b), $K_2 = 1.9 \times 10^6$ erg/cm$^3$ is used. For (c), $K_2 = 1.71 \times 10^6$ erg/cm$^3$ and $b_0 = K_1$ are used.

thermal conductivities increase with the spin chirality and result in the nonreciprocal thermal transport.

For the nonreciprocal thermal transport, we define the thermal rectification ratio:

$$r_{mag} = \frac{j^{heat}(\partial_x T > 0) - j^{heat}(\partial_x T < 0)}{j^{heat}(\partial_x T > 0) + j^{heat}(\partial_x T < 0)}. \quad (19)$$

Figure 5 shows the thermal rectification ratio for easy-cone ferromagnets and antiferromagnets for the linear temperature gradient, which increases as the chirality $\phi'a$ increases and is higher in antiferromagnets than in ferromagnets.

## V. DISCUSSION

We have shown that the injected spin current generates a chiral spin texture inside easy-cone ferromagnets and antiferromagnets and spin waves on top of it exhibit finite nonreciprocity. We note three features of the obtained nonreciprocal spin waves. First, the spin-wave nonreciprocity can be induced without an external field in easy-cone ferromagnets, in contrast to the previously known case of easy-plane ferromagnets where an external field is required [34–38]. Second, the nonreciprocity in spin waves is generated by electrically injecting chirality into nonchiral magnets and thus allows for dynamical manipulation. Last, due to the gapless nature of the nonreciprocal spin waves, the nonreciprocal thermal transport can be large at sufficiently low temperatures. We remark that the nonreciprocal spin-wave transport can also be examined by other methods such as spin-wave spectroscopy [6,7,18] and Brillouin light scattering [14,15].

We would like to discuss two issues related to the material realization. First, although the magnetic anisotropy parameters of the insulating easy-cone magnets are not characterized well, recent studies have shown that magnetic anisotropy is controllable using epitaxial strain in magnetic insulators [60,66,67], suggesting large tunability of material parameters for insulating magnets. Second, the spin-orbit coupling or dipolar interaction can violate the U(1) symmetry and generate in-plane magnetic anisotropy, by which the ground state

would be modified to an array of domain walls carrying a spin current [23,26,31,52,68,69]. It is expected that the spin-wave nonreciprocity can be induced in the array of domain walls, but the thermal-transport efficiency is suppressed exponentially with temperature due to the magnon gap.

We would also like to mention that the need to maintain the current in heavy metals (shown in Fig. 1 in our setup) to sustain the spin-wave nonreciprocity in our model can be obviated by replacing the heavy metals with metallic ferromagnets exhibiting a finite spin Hall effect [70–75] with easy-axis anisotropy along the $y$ axis, wherein the exchange field from the metallic magnet can fix the boundary magnetizations and thereby prevent the injected chiral texture from unwinding under favorable conditions.

## APPENDIX A: STEADY-STATE SOLUTION OF THE FERROMAGNET

Here, we discuss the dynamic steady state that carries a finite spin supercurrent. The classical dynamics of the unit vector is described by the Landau-Lifshitz-Gilbert equation

$$\dot{\mathbf{n}} + \alpha \mathbf{n} \times \dot{\mathbf{n}} = \frac{1}{s} \mathbf{n} \times (A \partial_x^2 \mathbf{n} + K_1 n_z \hat{\mathbf{z}} - 2K_2 n_z^3 \hat{\mathbf{z}}). \quad (A1)$$

In the spherical coordinate, we have

$$s \sin \theta \dot{\phi} + \alpha s \dot{\theta} = A\theta'' + [K_1 - K_2(1 + \cos 2\theta) + A(\phi')^2] \cos \theta \sin \theta,$$

$$s \sin \theta \dot{\theta} - \alpha s \sin^2 \theta \dot{\phi} = -A[(\sin^2 \theta)\phi']'. \quad (A2)$$

For the zero Gilbert damping case ($\alpha = 0$), the last line of Eq. (A2) is the continuity equation of the spin current density $J_z^s = -A \sin^2 \theta \phi'$ and the spin density $sn_z = s \cos \theta$ [30,54]. We are interested in the nonequilibrium steady state close to the ground state $\theta = \theta_c$ and $\phi' = 0$. A steady-state solution can be obtained by taking an ansatz such that $\theta(x, t) = \theta_c$. Then, from Eq. (A2), we have

$$\dot{\phi} = \frac{\cos \theta_c}{s}[K_1 - K_2(1 + \cos 2\theta_c) + A(\phi')^2] \equiv \Omega,$$

$$\phi'(x) = \frac{\alpha s}{A} \Omega x + \phi'(0), \quad (A3)$$

which leads to $\phi(x, t) = \phi(x) + \Omega t$. The effects of the spin current injection from sandwiching the magnet with heavy metals is captured by the boundary conditions [31,54]

$$(J_L^s)_z = \sin^2 \theta_c (j_L \vartheta - \gamma_L \Omega),$$
$$(J_R^s)_z = \sin^2 \theta_c (j_R \vartheta + \gamma_R \Omega), \qquad (A4)$$

where $\vartheta$ is the coefficient for the dampinglike torque, which is related to the effective interfacial spin Hall angle $\theta$ via $\vartheta \equiv \hbar \tan \theta / 2 e t_N$ [50], and $\gamma (\equiv \hbar g^{\uparrow\downarrow}/4\pi)$ is the renormalized spin-mixing conductance.

The loss of the spin supercurrent by spin dissipation in a ferromagnet of length $L$ is given by

$$\Delta J_z^s = (J_L^s)_z - (J_R^s)_z$$
$$= \sin^2 \theta_c [(j_L - j_R)\vartheta - (\gamma_L + \gamma_R)\Omega]. \qquad (A5)$$

This is equivalent to

$$\Delta J_s^z = -A \sin^2 \theta_c \left[\frac{\alpha s}{A} \Omega x\right]_L^0 = \alpha s \Omega L \sin^2 \theta_c. \qquad (A6)$$

By using Eqs. (A5) and (A6), we have

$$\Omega = \frac{(j_L - j_R)\vartheta}{2\gamma + \gamma_\alpha}, \qquad (A7)$$

where $\gamma_\alpha = \alpha s L$. The rotation frequency depends on the electrical circuit configuration. For a series configuration, $j_R = -j_L$; then

$$\Omega_{\text{series}} = \frac{j\vartheta}{\gamma + \gamma_\alpha/2}. \qquad (A8)$$

For a parallel configuration, $j_R = j_L = j$; then

$$\Omega_{\text{parallel}} = 0. \qquad (A9)$$

In the parallel configuration ($\Omega = 0$), from the last line of Eq. (A2) and the first line of Eq. (A4), we have

$$(J_L^s)_z = -A \sin^2 \theta_c \phi' = \sin^2 \theta_c j\vartheta, \qquad (A10)$$

which leads to $\phi'(x) = -\frac{j\vartheta}{A} \equiv \phi'$. Also, from Eq. (A3), we obtain the quasiequilibrium angle

$$\theta_c = \frac{1}{2} \cos^{-1} \left(\frac{K_1 - K_2 + A(\phi')^2}{K_2}\right). \qquad (A11)$$

Note that the effect of $\phi'$ renormalizes $K_1$ to $K_1 + A(\phi')^2$.

## APPENDIX B: SPIN-WAVE DISPERSION CONTINUUM MODEL DESCRIPTION

### 1. Easy-cone ferromagnet

We start from the continuum model Hamiltonian of the easy-cone ferromagnet

$$H = \int d^3x \{A[\nabla \mathbf{n}(x)]^2 - K_1 n_z(x)^2 + K_2 n_z(x)^2\}/2, \qquad (B1)$$

where $K_1(> 0)$ is the easy-axis anisotropy and $K_2(> 0)$ is the second-order anisotropy. The static spin texture is $\mathbf{n}_0(x) = s(\sin \theta_c \cos \phi(x), \sin \theta_c \sin \phi(x), \cos \theta_c)$, where $\phi(x) = \phi_0 + \phi'x$. To investigate the spin-wave dynamics on the static spin texture, we divide $\mathbf{n}$ into the static profile $\mathbf{n}_0(x)$ and the small spin fluctuations $\delta \mathbf{n}$. Then we have following equation of motion:

$$\delta \dot{\mathbf{n}} = -\frac{1}{s}(\mathbf{n}_0 + \delta \mathbf{n}) \times \left[-A\partial_x^2(\mathbf{n}_0 + \delta \mathbf{n}) - K_1(n_{0,z} + \delta n_z)\hat{\mathbf{z}} + 2K_2(n_{0,z} + \delta n_z)^3\hat{\mathbf{z}}\right]. \qquad (B2)$$

In the spherical coordinates, we have

$$\delta \mathbf{n} = n^\theta \hat{\boldsymbol{\theta}} + n^\phi \hat{\boldsymbol{\phi}}, \quad \delta n_z = -\sin \theta_c n_\theta, \quad \hat{\mathbf{z}} = \cos \theta_c \hat{\mathbf{n}} - \sin \theta_c \hat{\boldsymbol{\theta}}. \qquad (B3)$$

Applying the steady-state solution $\theta' = \theta'' = 0$, $\phi'' = 0$, we have

$$-A(\phi')^2 - K_1 + 2K_2 \cos^2 \theta_c = 0 \qquad (B4)$$

and

$$s\dot{n}_\theta = -An_\phi'' - 2A \cos \theta_c \phi' n_\theta' + A \cos^2 \theta_c (\phi')^2 n_\phi + K_1 \cos^2 \theta_c n_\phi - 2K_2 \cos^4 \theta_c n_\phi,$$
$$s\dot{n}_\phi = An_\theta'' - 2A \cos \theta_c \phi' n_\phi' - A \cos(2\theta_c)(\phi')^2 n_\theta - K_1 \cos 2\theta_c n_\theta + 2K_2 \cos^4 \theta_c n_\theta - 6K_2 \sin^2 \theta_c \cos^2 \theta_c. \qquad (B5)$$

The zeroth-order equation [Eq. (B4)] describes the quasiequilibrium profile

$$\theta_c = \frac{1}{2} \cos^{-1} \left[\frac{\bar{K}_1 - K_2}{K_2}\right], \qquad (B6)$$

where $\bar{K}_1 = K_1 + A(\phi')^2$ is the renormalized easy-axis anisotropy. Inserting Eq. (B6) into Eq. (B5), we have

$$s\dot{n}_\theta = -An_\phi'' - A\sqrt{\frac{2\bar{K}_1}{K_2}} \phi' n_\theta',$$

$$s\dot{n}_\phi = An_\theta'' - K_{\phi'} n_\theta - A\sqrt{\frac{2\bar{K}_1}{K_2}} \phi' n_\phi', \qquad (B7)$$

where $K_{\phi'} = \bar{K}_1(2K_2 - \bar{K}_1)/K_2$. Inserting $n \propto e^{i(kx-\omega t)}$, we have

$$-is\omega n_\theta = Ak^2 n_\phi - ik\left(A\sqrt{\frac{2\bar{K}_1}{K_2}}\phi'\right)n_\theta$$

$$-is\omega n_\phi = -(Ak^2 + K_{\phi'})n_\theta - ik\left(A\sqrt{\frac{2\bar{K}_1}{K_2}}\phi'\right)n_\phi. \tag{B8}$$

In a simplified form, we write

$$-is\omega' n_\theta = Cn_\phi, \quad -is\omega' n_\phi = -Dn_\theta, \tag{B9}$$

where $s\omega' = s\omega - k(A\sqrt{\frac{2\bar{K}_1}{K_2}}\phi')$ and

$$C = Ak^2, \quad D = Ak^2 + K_{\phi'}. \tag{B10}$$

Thus, we obtain

$$s\omega' = \sqrt{CD} \quad \rightarrow \quad s\omega = \sqrt{Ak^2[Ak^2 + K_{\phi'}]} + k\left(A\sqrt{\frac{2\bar{K}_1}{K_2}}\phi'\right). \tag{B11}$$

### 2. Easy-cone antiferromagnet

The effective Lagrangian density of the easy-cone antiferromagnet is [30]

$$\mathcal{L}_{AFM} = s\mathbf{m} \cdot (\mathbf{n} \times \dot{\mathbf{n}}) - \frac{A}{2}(\partial_i \mathbf{n})^2 - \frac{\mathbf{m}^2}{2\chi} + \frac{K_1}{2}n_z^2 - \frac{K_2}{2}n_z^4 - \mathbf{b} \cdot \mathbf{m}, \tag{B12}$$

where $\mathbf{n}$ and $\mathbf{m}$ are the two slow continuum fields, which parametrize the staggered (Néel) and smooth (magnetic) components of the spins, respectively. $\chi = \frac{a^2}{A}$ is the spin susceptibility, $A$ is the exchange stiffness of the Néel order, $K_1 > 0$ and $K_2 > 0$ are the first- and second-order anisotropy energy densities, and $\mathbf{b}$ is the external magnetic field. By minimizing the action with two constraints, $|\mathbf{n}| = 1$ and $\mathbf{n} \cdot \mathbf{m} = 0$, we obtain the equations of motion

$$s\dot{\mathbf{n}} = \frac{1}{\chi}(\mathbf{m} \times \mathbf{n}) + \mathbf{b} \times \mathbf{n},$$

$$s\dot{\mathbf{m}} = A\mathbf{n} \times \nabla^2 \mathbf{n} + K_1 n_z(\mathbf{n} \times \hat{\mathbf{z}}) - 2K_2 n_z^3(\mathbf{n} \times \hat{\mathbf{z}}) + \mathbf{b} \times \mathbf{m}. \tag{B13}$$

Since $|\mathbf{n}| = 1$ and $\mathbf{n} \cdot \mathbf{m} = 0$, we can choose $\mathbf{n} = \hat{n}$, $\mathbf{m} = m_\theta \hat{\theta} + m_\phi \hat{\phi}$. In Cartesian coordinates, we have $\mathbf{n} = (\sin\theta\cos\phi, \sin\theta\sin\phi, \cos\theta)$ and $\mathbf{m} = (m_\theta\cos\theta\cos\phi - m_\phi\sin\phi, m_\phi\cos\phi + m_\theta\cos\theta\sin\phi, -m_\theta\sin\theta)$.

For $\mathbf{b} = -b_0\hat{\mathbf{z}}$, we have the equilibrium solution of the uniform state:

$$m_\theta = -\chi b_0 \sin\theta, \quad m_\phi = 0, \quad \theta_c = \frac{1}{2}\cos^{-1}\left(\frac{K_1 - K_2 - b_0^2\chi}{K_2}\right). \tag{B14}$$

When the spin currents are injected from the left and right leads (parallel configuration), we have the static texture of the Néel vector: $\mathbf{n}_0(x) = s(\sin\theta_c\cos\phi(x), \sin\theta_c\sin\phi(x), \cos\theta_c)$, where $\phi(x) = \phi_0 + \phi'x$. In this case, the equilibrium solution is modified as

$$m_\theta = -\chi b_0 \sin\theta, \quad m_\phi = 0, \quad \theta_c = \frac{1}{2}\cos^{-1}\left(\frac{K_1 + A(\phi_0')^2 - K_2 - b_0^2\chi}{K_2}\right). \tag{B15}$$

Note that $\phi'$ renormalizes $K_1$ to $\bar{K}_1 = K_1 + A(\phi')^2$. To obtain the spin-wave solution, we consider small deviations from the equilibrium solution:

$$m_\theta = -\chi b_0 \sin\theta + \xi_\theta, \quad m_\phi = \xi_\phi, \quad \theta = \theta_c + \delta\theta, \quad \phi = \phi_0(x) + \delta\phi. \tag{B16}$$

Expanding Eq. (B13) up to linear order in $\xi_\theta, \xi_\phi, \delta\theta$, and $\delta\phi$, we have

$$s\dot{\delta\theta} = \chi^{-1}\xi_\phi, \quad s\dot{\delta\phi} = -\frac{\xi_\theta}{\chi\sin\theta_c} - b_0\cot\theta_c\delta\theta,$$

$$s\dot{\xi_\theta} = -A\sin\theta_c\nabla^2\delta\phi - 2A\cos\theta_c\phi'\partial_x(\delta\theta) + b_0\cos\theta_c\xi_\phi,$$

$$s\dot{\xi_\phi} = A\nabla^2\delta\theta - A\sin(2\theta_c)\phi'\partial_x(\delta\phi) - 2b_0\cos\theta_c\xi_\theta - \kappa_{\phi'}\delta\theta, \tag{B17}$$

where

$$\kappa_{\phi'} = \frac{(\bar{K}_1 - \chi b_0^2)[2(K_2 + \chi b_0^2) - \bar{K}_1]}{K_2}. \tag{B18}$$

Replacing $\delta\phi$ with $\delta\phi/\sin\theta_c$, we have

$$s\dot{\delta\theta} = \chi^{-1}\xi_\phi, \quad s\dot{\delta\phi} = -\chi^{-1}\xi_\theta - b_0 n_z^{\text{eq}}\,\delta\theta,$$

$$s\dot{\xi_\theta} = -A\nabla^2\delta\phi - 2An_z^{\text{eq}}\,\phi'\partial_x(\delta\theta) + b_0 n_z^{\text{eq}}\,\xi_\phi,$$

$$s\dot{\xi_\phi} = A\nabla^2\delta\theta - 2An_z^{\text{eq}}\,\phi'\partial_x(\delta\phi) - 2b_0 n_z^{\text{eq}}\,\xi_\theta - \kappa_{\phi'}\delta\theta, \tag{B19}$$

where $n_z^{\text{eq}} = \cos\theta_c$. Applying $\psi \sim \psi e^{i(kx-\omega t)}$, we obtain

$$-is\omega\delta\theta = \chi^{-1}\xi_\phi, \quad -is\omega\delta\phi = -\chi^{-1}\xi_\theta - b_0 n_z^{\text{eq}}\,\delta\theta,$$

$$-is\omega\xi_\theta = Ak^2\delta\phi - 2ikAn_z^{\text{eq}}\,\phi'\delta\theta + b_0 n_z^{\text{eq}}\,\xi_\phi,$$

$$-is\omega\xi_\phi = -Ak^2\delta\theta - 2ikAn_z^{\text{eq}}\,\phi'\delta\phi - 2b_0 n_z^{\text{eq}}\,\xi_\theta - \kappa_{\phi'}\delta\theta. \tag{B20}$$

Then,

$$\omega\begin{pmatrix}\delta\theta\\\xi_\phi\\\delta\phi\\\xi_\theta\end{pmatrix} = \frac{i}{s}\begin{pmatrix}0 & \chi^{-1} & 0 & 0\\-Ak^2-\kappa_{\phi'} & 0 & -2ikAn_z^{\text{eq}}\,\phi' & -2b_0 n_z^{\text{eq}}\\-b_0 n_z^{\text{eq}} & 0 & 0 & -\chi^{-1}\\-2ikAn_z^{\text{eq}}\,\phi' & b_0 n_z^{\text{eq}} & Ak^2 & 0\end{pmatrix}\begin{pmatrix}\delta\theta\\\xi_\phi\\\delta\phi\\\xi_\theta\end{pmatrix}. \tag{B21}$$

## APPENDIX C: HOLSTEIN-PRIMAKOFF MAGNON DESCRIPTION

### 1. Easy-cone ferromagnet

The lattice model Hamiltonian for the easy-cone ferromagnet under the magnetic field is

$$H = -J\sum_i \mathbf{S}_i \cdot \mathbf{S}_{i+1} - \frac{K_1}{2}\sum_i (S_i^z)^2 + \frac{K_2}{2}\sum_i (S_i^z)^4 - b\sum_i S_i^z. \tag{C1}$$

Let $a$ be a lattice constant. When the spin texture is given by $\mathbf{S}_{0,i} = S(\sin\theta_0\cos\phi_i, \sin\theta_0\sin\phi_i, \cos\theta_0)$, with $\phi_i = (\phi'a)i + \phi_0$, the quasiequilibrium polar angle $\theta_0$ can be obtained by minimizing

$$\frac{H}{N} = -JS^2[\sin^2\theta_0\cos(\phi'a) + \cos^2\theta_0] - \frac{K_1}{2}S^2\cos^2\theta_0 + \frac{K_2}{2}S^4\cos^4\theta_0 - bS\cos\theta_0, \tag{C2}$$

where $N$ is the total number of spins.

To examine a small spin fluctuation in the quasiequilibrium spins, it is convenient to introduce local primed coordinate systems for each spin in which the spins are along the $z'$ axis. That is, $\mathbf{S}'_{0,i} = R_i\mathbf{S}_{0,i} = S(0,0,1)^T$, where

$$R_i = R_y(-\theta_0)R_z(-\phi_i) = \begin{pmatrix}\cos\theta_0\cos\phi_i & \cos\theta_0\sin\phi_i & -\sin\theta_0\\-\sin\phi_i & \cos\phi_i & 0\\\sin\theta_0\cos\phi_i & \sin\theta_0\sin\phi_i & \cos\theta_0\end{pmatrix}. \tag{C3}$$

We can get the Hamiltonian in the new coordinate system by substituting $\mathbf{S}_{0,i} = R_i^{-1}\mathbf{S}'_{0,i}$ into $H$. We neglect the $S'_x, S'_y, S'_x S'_z$, and $S'_y S'_z$ terms, which do not contribute to the spin-wave dynamics.

We can apply the Holstein-Primakoff transformation with the large-$S$ limit to examine the low-energy physics:

$$S_{i,x}'^A = \sqrt{\frac{S}{2}}(a_i^\dagger + a_i), \quad S_{i,y}'^A = i\sqrt{\frac{S}{2}}(a_i^\dagger - a_i), \quad S_{i,z}'^A = S - a_i^\dagger a_i, \tag{C4}$$

where $a$ and $b$ are bosonic operators. After employing the Holstein-Primakoff transformation and the Fourier transformation $a_i = \frac{1}{\sqrt{N}} \sum_{\mathbf{k}} a_{\mathbf{k}} e^{i\mathbf{k}\cdot\mathbf{r}_i}$, we get

$$H = \sum_{\mathbf{k}} \left\{ A_k a_{\mathbf{k}}^{\dagger} a_{\mathbf{k}} + \frac{1}{2} B_{\mathbf{k}} a_{\mathbf{k}}^{\dagger} a_{-\mathbf{k}}^{\dagger} + \frac{1}{2} B_{\mathbf{k}}^* a_{\mathbf{k}} a_{-\mathbf{k}} \right\}, \tag{C5}$$

where

$$A_{\mathbf{k}} = \cos\theta_0 (b + 2JS \sin k_x a \, \sin\phi' a) - JS \cos k_x a \, [\cos\phi' a \, (1 + \cos^2\theta_0) + \sin^2\theta_0]$$
$$+ \tfrac{1}{8} S\{8J + 2K_1 - 3K_2 S^2 + (8J + 6K_1 - 8K_2 S^2) \cos 2\theta_0 - 5K_2 S^2 \cos 4\theta_0 + 16J \cos\phi' a \, \sin^2\theta_0\}$$
$$B_{\mathbf{k}} = \tfrac{1}{2} S \sin^2\theta_0 \{-K_1 + 3K_2 S^2 + 2e^{ik_x a} J(\cos\phi' a - 1) + 3K_2 S^2 \cos 2\theta_0\}. \tag{C6}$$

We now have to perform the Bogoliubov transformation. First, let us introduce $\psi_{\mathbf{k}} = (a_{\mathbf{k}}, a_{-\mathbf{k}}^{\dagger})^T$ and rewrite $\mathcal{H}_{\mathbf{k}}$ in matrix form: $H = \frac{1}{2} \sum_{\mathbf{k}} \psi_{\mathbf{k}}^{\dagger} \mathcal{H}_{\mathbf{k}} \psi_{\mathbf{k}}$, where $\mathcal{H}_{\mathbf{k}} = \begin{pmatrix} A_{\mathbf{k}} & B_{\mathbf{k}} \\ B_{\mathbf{k}}^* & A_{-\mathbf{k}} \end{pmatrix}$. Let $J = \begin{pmatrix} 1 & 0 \\ 0 & -1 \end{pmatrix}$. It is known that when $\mathcal{H}_{\mathbf{k}}$ is positive definite, if we denote the two eigenvalues of $J\mathcal{H}_{\mathbf{k}}$ by $\epsilon_{\mathbf{k},1}$ and $\epsilon_{\mathbf{k},2}$, then $\epsilon_{\mathbf{k},1} = -\epsilon_{\mathbf{k},2} > 0$, and the eigenvalues of $\mathcal{H}_{\mathbf{k}}$ are given by $\epsilon_{\mathbf{k},1} - \epsilon_{-\mathbf{k},2}$. Since $\epsilon_{\mathbf{k},1/2} = \frac{1}{2}(A_{\mathbf{k}} - A_{-\mathbf{k}} \pm \sqrt{(A_{\mathbf{k}} + A_{-\mathbf{k}})^2 - 4|B_{\mathbf{k}}|^2})$, the magnon dispersion relation is given by $\hbar\omega = \frac{1}{2}(A_{\mathbf{k}} - A_{-\mathbf{k}} + \sqrt{(A_{\mathbf{k}} + A_{-\mathbf{k}})^2 - 4|B_{\mathbf{k}}|^2})$.

### 2. Easy-cone antiferromagnet

The lattice model Hamiltonian for the easy-cone antiferromagnet is

$$H = J \sum_i \mathbf{S}_i \cdot \mathbf{S}_{i+1} - \frac{K_1}{2} \sum_i (S_i^z)^2 + \frac{K_2}{2} \sum_i (S_i^z)^4 - b \sum_i S_i^z. \tag{C7}$$

Here, we assume that the lattice is bipartite, i.e., has two sublattices, A and B. When a spin texture is given by $\mathbf{S}_{0,i} = S(\sin\theta_0 \cos\phi_i, \sin\theta_0 \sin\phi_i, \cos\theta_0)$, with $\phi_i = (\phi' a)i + \phi_0$, the quasiequilibrium polar angles $\theta_A$ and $\theta_B$ on each sublattice can be obtained by minimizing

$$\frac{H}{N} = 2JS^2 (\sin\theta_A \sin\theta_B \cos\Delta\phi + \cos\theta_A \cos\theta_B) - \frac{K_1}{2} S^2 (\cos^2\theta_A + \cos^2\theta_B)$$
$$+ \frac{K_2}{2} S^4 (\cos^4\theta_A + \cos^4\theta_B) - bS(\cos\theta_A + \cos\theta_B), \tag{C8}$$

where $N$ is the total number of spins in each sublattice.

We introduce the local coordinate systems in which the spins are along the $z'$ axis. Here, we have to rotate separately the spins of each sublattice $A$ and $B$ by the polar angles $\theta_A$ and $\theta_B$, respectively. Next, we apply the Holstein-Primakoff transformation with two independent bosonic species, $a_i$ for $i \in A$ and $b_i$ for $i \in B$:

$$S_{i,x}'^A = \sqrt{\frac{S}{2}}(a_i^{\dagger} + a_i), \quad S_{i,y}'^A = i\sqrt{\frac{S}{2}}(a_i^{\dagger} - a_i), \quad S_{i,z}'^A = S - a_i^{\dagger} a_i,$$

$$S_{i,x}'^B = \sqrt{\frac{S}{2}}(b_i^{\dagger} + b_i), \quad S_{i,y}'^B = i\sqrt{\frac{S}{2}}(b_i^{\dagger} - b_i), \quad S_{i,z}'^B = S - b_i^{\dagger} b_i. \tag{C9}$$

After employing the Holstein-Primakoff transformation and the Fourier transformation $a_i = \frac{1}{\sqrt{N}} \sum_{\mathbf{k}} a_{\mathbf{k}} e^{i\mathbf{k}\cdot\mathbf{r}_i}$ and $b_i = \frac{1}{\sqrt{N}} \sum_{\mathbf{k}} b_{\mathbf{k}} e^{i\mathbf{k}\cdot\mathbf{r}_i}$, we obtain

$$H = \sum_{\mathbf{k}} \{ A a_{\mathbf{k}}^{\dagger} a_{\mathbf{k}} + B b_{\mathbf{k}}^{\dagger} b_{\mathbf{k}} + C_{\mathbf{k}}(a_{\mathbf{k}} b_{-\mathbf{k}} + a_{\mathbf{k}}^{\dagger} b_{-\mathbf{k}}^{\dagger}) + D_{\mathbf{k}}(a_{\mathbf{k}}^{\dagger} b_{\mathbf{k}} + a_{\mathbf{k}} b_{\mathbf{k}}^{\dagger}) + E(a_{\mathbf{k}} a_{-\mathbf{k}} + a_{\mathbf{k}}^{\dagger} a_{-\mathbf{k}}^{\dagger}) + F(b_{\mathbf{k}} b_{-\mathbf{k}} + b_{\mathbf{k}}^{\dagger} b_{-\mathbf{k}}^{\dagger}) \}, \tag{C10}$$

where

$$A = -2K_2 S^3 \cos^4\theta_A + (b - 2JS \cos\theta_B) \cos\theta_A + S(K1 + 3K_2 S^2 \sin^2\theta_A) \cos^2\theta_A$$
$$- \tfrac{1}{2} S \sin\theta_A (K_1 \sin\theta_A + 4J \cos\Delta\phi \sin\theta_B),$$
$$B = -2K_2 S^3 \cos^4\theta_B + (b - 2JS \cos\theta_A) \cos\theta_B + S(K1 + 3K_2 S^2 \sin^2\theta_B) \cos^2\theta_B$$
$$- \tfrac{1}{2} S \sin\theta_B (K_1 \sin\theta_B + 4J \cos\Delta\phi \sin\theta_A),$$
$$C_{\mathbf{k}} = JS\{(\cos\theta_A - \cos\theta_B) \sin k_x a \, \sin\Delta\phi + \cos k_x a \, [\cos\Delta\phi(\cos\theta_A \cos\theta_B - 1) + \sin\theta_A \sin\theta_B]\},$$
$$D_{\mathbf{k}} = JS\{-(\cos\theta_A + \cos\theta_B) \sin k_x a \, \sin\Delta\phi + \cos k_x a \, [\cos\Delta\phi(\cos\theta_A \cos\theta_B + 1) + \sin\theta_A \sin\theta_B]\},$$
$$E = \tfrac{1}{4} S(-K_1 + 6K_2 S^2 \cos^2\theta_A) \sin^2\theta_A,$$
$$F = \tfrac{1}{4} S(-K_1 + 6K_2 S^2 \cos^2\theta_B) \sin^2\theta_B. \tag{C11}$$

Let us introduce $\psi_{\mathbf{k}} = (a_{\mathbf{k}}, b_{\mathbf{k}}, a_{-\mathbf{k}}^{\dagger}, b_{-\mathbf{k}}^{\dagger})^T$. The Hamiltonian then can be written in matrix form: $H = \frac{1}{2}\sum_{\mathbf{k}} \psi_{\mathbf{k}}^{\dagger} \mathcal{H}_{\mathbf{k}} \psi_{\mathbf{k}}$, where

$$\mathcal{H}_{\mathbf{k}} = \begin{pmatrix} A & D_{\mathbf{k}} & 2E & C_{\mathbf{k}} \\ D_{\mathbf{k}} & B & C_{-\mathbf{k}} & 2F \\ 2E & C_{-\mathbf{k}} & A & D_{-\mathbf{k}} \\ C_{\mathbf{k}} & 2F & D_{-\mathbf{k}} & B \end{pmatrix}. \tag{C12}$$

When $\mathcal{H}_{\mathbf{k}}$ is positive definite, we can use the same $J$ matrix that we used for the easy-cone ferromagnet. In this case, $J = \begin{pmatrix} I_{2\times 2} & 0 \\ 0 & -I_{2\times 2} \end{pmatrix}$. If we denote the eigenvalues of $J\mathcal{H}_{\mathbf{k}}$ by $\epsilon_{\mathbf{k},1}, \epsilon_{\mathbf{k},2}, \epsilon_{\mathbf{k},3}$, and $\epsilon_{\mathbf{k},4}$ in descending order, the two magnon bands are then given by $\frac{1}{2}(\epsilon_{\mathbf{k},1} - \epsilon_{-\mathbf{k},4})$ and $\frac{1}{2}(\epsilon_{\mathbf{k},2} - \epsilon_{-\mathbf{k},3})$.

---

[1] Y. Tokura and N. Nagaosa, Nat. Commun. **9**, 3740 (2018).

[2] S. Cheon, H.-W. Lee, and S.-W. Cheong, Phys. Rev. B **98**, 184405 (2018).

[3] S.-W. Cheong, D. Talbayev, V. Kiryukhin, and A. Saxena, npj Quantum Mater. **3**, 19 (2018).

[4] M. Jamali, J. H. Kwon, S.-M. Seo, K.-J. Lee, and H. Yang, Sci. Rep. **3**, 3160 (2013).

[5] A. V. Chumak, V. I. Vasyuchka, A. A. Serga, and B. Hillebrands, Nat. Phys. **11**, 453 (2015).

[6] V. Vlaminck and M. Bailleul, Science **322**, 410 (2008).

[7] V. Vlaminck and M. Bailleul, Phys. Rev. B **81**, 014425 (2010).

[8] K. Sekiguchi, K. Yamada, S.-M. Seo, K.-J. Lee, D. Chiba, K. Kobayashi, and T. Ono, Phys. Rev. Lett. **108**, 017203 (2012).

[9] D.-H. Kim, S.-H. Oh, D.-K. Lee, S. K. Kim, and K.-J. Lee, Phys. Rev. B **103**, 014433 (2021).

[10] T. An, V. I. Vasyuchka, K. Uchida, A. V. Chumak, K. Yamaguchi, K. Harii, J. Ohe, M. B. Jungfleisch, Y. Kajiwara, H. Adachi, B. Hillebrands, S. Maekawa, and E. Saitoh, Nat. Mater. **12**, 549 (2013).

[11] R. L. Melcher, Phys. Rev. Lett. **30**, 125 (1973).

[12] M. Kataoka, J. Phys. Soc. Jpn. **56**, 3635 (1987).

[13] J.-H. Moon, S.-M. Seo, K.-J. Lee, K.-W. Kim, J. Ryu, H.-W. Lee, R. D. McMichael, and M. D. Stiles, Phys. Rev. B **88**, 184404 (2013).

[14] K. Di, V. L. Zhang, H. S. Lim, S. C. Ng, M. H. Kuok, J. Yu, J. Yoon, X. Qiu, and H. Yang, Phys. Rev. Lett. **114**, 047201 (2015).

[15] K. Di, V. L. Zhang, H. S. Lim, S. C. Ng, M. H. Kuok, X. Qiu, and H. Yang, Appl. Phys. Lett. **106**, 052403 (2015).

[16] T. Kikuchi, T. Koretsune, R. Arita, and G. Tatara, Phys. Rev. Lett. **116**, 247201 (2016).

[17] Y. Iguchi, S. Uemura, K. Ueno, and Y. Onose, Phys. Rev. B **92**, 184419 (2015).

[18] S. Seki, Y. Okamura, K. Kondou, K. Shibata, M. Kubota, R. Takagi, F. Kagawa, M. Kawasaki, G. Tatara, Y. Otani, and Y. Tokura, Phys. Rev. B **93**, 235131 (2016).

[19] S. Seki, M. Garst, J. Waizner, R. Takagi, N. D. Khanh, Y. Okamura, K. Kondou, F. Kagawa, Y. Otani, and Y. Tokura, Nat. Commun. **11**, 256 (2020).

[20] N. Ogawa, L. Köhler, M. Garst, S. Toyoda, S. Seki, and Y. Tokura, Proc. Natl. Acad. Sci. USA **118**, e2022927118 (2021).

[21] A. V. Chumak, P. Dhagat, A. Jander, A. A. Serga, and B. Hillebrands, Phys. Rev. B **81**, 140404(R) (2010).

[22] T. Yu, C. Wang, M. A. Sentef, and G. E. W. Bauer, Phys. Rev. Lett. **126**, 137202 (2021).

[23] E. B. Sonin, Adv. Phys. **59**, 181 (2010).

[24] J. König, M. C. Bønsager, and A. H. MacDonald, Phys. Rev. Lett. **87**, 187202 (2001).

[25] W. Chen and M. Sigrist, Phys. Rev. B **89**, 024511 (2014).

[26] A. Qaiumzadeh, H. Skarsvåg, C. Holmqvist, and A. Brataas, Phys. Rev. Lett. **118**, 137201 (2017).

[27] M. Evers and U. Nowak, Phys. Rev. B **101**, 184415 (2020).

[28] S. K. Kim and Y. Tserkovnyak, Phys. Rev. B **94**, 220404(R) (2016).

[29] R. Zarzuela, D. Hill, J. Sinova, and Y. Tserkovnyak, Phys. Rev. B **103**, 174424 (2021).

[30] S. Takei, B. I. Halperin, A. Yacoby, and Y. Tserkovnyak, Phys. Rev. B **90**, 094408 (2014).

[31] S. Takei and Y. Y. Tserkovnyak, Phys. Rev. Lett. **115**, 156604 (2015).

[32] W. Yuan, Q. Zhu, T. Su, Y. Yao, W. Xing, Y. Chen, Y. Ma, X. Lin, J. Shi, R. Shindou, X. C. Xie, and W. Han, Sci. Adv. **4**, eaat1098 (2018).

[33] P. Stepanov, S. Che, D. Shcherbakov, J. Yang, R. Chen, K. Thilahar, G. Voigt, M. W. Bockrath, D. Smirnov, K. Watanabe, T. Taniguchi, R. K. Lake, Y. Barlas, A. H. MacDonald, and C. N. Lau, Nat. Phys. **14**, 907 (2018).

[34] E. Iacocca, T. J. Silva, and M. A. Hoefer, Phys. Rev. Lett. **118**, 017203 (2017).

[35] E. Iacocca and M. A. Hoefer, Phys. Rev. B **95**, 134409 (2017).

[36] E. Iacocca and M. A. Hoefer, Phys. Lett. A **383**, 125858 (2019).

[37] E. B. Sonin, Phys. Rev. B **97**, 224517 (2018).

[38] E. B. Sonin, Phys. Rev. B **99**, 104423 (2019).

[39] G. Yu, P. Upadhyaya, Y. Fan, J. G. Alzate, W. Jiang, K. L. Wong, S. Takei, S. A. Bender, L.-T. Chang, Y. Jiang, M. Lang, J. Tang, Y. Wang, Y. Tserkovnyak, P. K. Amiri, and K. L. Wang, Nat. Nanotechnol. **9**, 548 (2014).

[40] A. van den Brink, G. Vermijs, A. Solignac, J. Koo, J. T. Kohlhepp, H. J. M. Swagten, and B. Koopmans, Nat. Commun. **7**, 10854 (2016).

[41] S. Fukami, C. Zhang, S. DuttaGupta, A. Kurenkov, and H. Ohno, Nat. Mater. **15**, 535 (2016).

[42] Y.-C. Lau, D. Betto, K. Rode, J. M. D. Coey, and P. Stamenov, Nat. Nanotechnol. **11**, 758 (2016).

[43] Y.-W. Oh, S.-H. C. Baek, Y. M. Kim, H. Y. Lee, K.-D. Lee, C.-G. Yang, E.-S. Park, K.-S. Lee, K.-W. Kim, G. Go, J.-R. Jeong, B.-C. Min, H.-W. Lee, K.-J. Lee, and B.-G. Park, Nat. Nanotechnol. **11**, 878 (2016).

[44] A. Kohen, Th. Proslier, T. Cren, Y. Noat, W. Sacks, H. Berger, and D. Roditchev, Phys. Rev. Lett. **97**, 027001 (2006).

[45] P.-H. Jang, S.-H. Oh, S. K. Kim, and K.-J. Lee, Phys. Rev. B **99**, 024424 (2019).

[46] H. Stillrich, C. Menk, R. Frömter, and H. P. Oepen, J. Appl. Phys. **105**, 07C308 (2009).

[47] J. M. Shaw, H. T. Nembach, M. Weiler, T. J. Silva, M. Schoen, J. Z. Sun, and D. C. Worledge, IEEE Magn. Lett. **6**, 1 (2015).

[48] O. Yamada, H. Tokuhara, F. Ono, M. Sagawa, and Y. Matsuura, J. Magn. Magn. Mater. **54–57**, 585 (1986).

[49] P. Schobinger-Papamantellos, C. Ritter, and K. H. J. Buschow, J. Magn. Magn. Mater. **260**, 156 (2003).

[50] Y. Tserkovnyak and S. A. Bender, Phys. Rev. B **90**, 014428 (2014).

[51] L. D. Landau, Zh. Eksp. Teor. Fiz. **11**, 592 (1941).

[52] E. Iacocca, T. J. Silva, and M. A. Hoefer, Phys. Rev. B **96**, 134434 (2017).

[53] H. Chen, A. D. Kent, A. H. MacDonald, and I. Sodemann, Phys. Rev. B **90**, 220401(R) (2014).

[54] S. K. Kim, S. Takei, and Y. Tserkovnyak, Phys. Rev. B **93**, 020402(R) (2016).

[55] S. Klingler, A. V. Chumak, T. Mewes, B. Khodadadi, C. Mewes, C. Dubs, O. Surzhenko, B. Hillebrands, and A. Conca, J. Phys. D **48**, 015001 (2015).

[56] G. Li, H. Bai, J. Su, Z. Z. Zhu, Y. Zhang, and J. W. Cai, APL Mater. **7**, 041104 (2019).

[57] C.-F. Pai, L. Liu, Y. Li, H. W. Tseng, D. C. Ralph, and R. A. Buhrman, Appl. Phys. Lett. **101**, 122404 (2012).

[58] S. Lee, S. Grudichak, J. Sklenar, C. C. Tsai, M. Jang, Q. Yang, H. Zhang, and J. B. Ketterson, J. Appl. Phys. **120**, 033905 (2016).

[59] J. Fu, M. Hua, X. Wen, M. Xue, S. Ding, M. Wang, P. Yu, S. Liu, J. Han, C. Wang, H. Du, Y. Yang, and J. Yang, Appl. Phys. Lett. **110**, 202403 (2017).

[60] Y. Lin, L. Jin, H. Zhang, Z. Zhong, Q. Yang, Y. Rao, and M. Li, J. Magn. Magn. Mater. **496**, 165886 (2020).

[61] K. M. D. Hals, Y. Tserkovnyak, and A. Brataas, Phys. Rev. Lett. **106**, 107206 (2011).

[62] R. Nakai and N. Nagaosa, Phys. Rev. B **99**, 115201 (2019).

[63] Y. Hirokane, Y. Nii, H. Masuda, and Y. Onose, Sci. Adv. **6**, eabd3703 (2020).

[64] B. Flebus, S. A. Bender, Y. Tserkovnyak, and R. A. Duine, Phys. Rev. Lett. **116**, 117201 (2016).

[65] M. Sparks, R. Loudon, and C. Kittel, Phys. Rev. **122**, 791 (1961).

[66] C. T. Wang, X. F. Liang, Y. Zhang, X. Liang, Y. P. Zhu, J. Qin, Y. Gao, B. Peng, N. X. Sun, and L. Bi, Phys. Rev. B **96**, 224403 (2017).

[67] L. Soumah, N. Beaulieu, L. Qassym, C. Carrétéro, E. Jacquet, R. Lebourgeois, J. B. Youssef, P. Bortolotti, V. Cros, and A. Anane, Nat. Commun. **9**, 3355 (2018).

[68] H. Skarsvåg, C. Holmqvist, and A. Brataas, Phys. Rev. Lett. **115**, 237201 (2015).

[69] D. Hill, S. K. Kim, and Y. Tserkovnyak, Phys. Rev. Lett. **121**, 037202 (2018).

[70] B. F. Miao, S. Y. Huang, D. Qu, and C. L. Chien, Phys. Rev. Lett. **111**, 066602 (2013).

[71] A. Tsukahara, Y. Ando, Y. Kitamura, H. Emoto, E. Shikoh, M. P. Delmo, T. Shinjo, and M. Shiraishi, Phys. Rev. B **89**, 235317 (2014).

[72] G. Qu, K. Nakamura, and M. Hayashi, Phys. Rev. B **102**, 144440 (2020).

[73] V. P. Amin, J. Li, M. D. Stiles, and P. M. Haney, Phys. Rev. B **99**, 220405(R) (2019).

[74] K.-W. Kim and K.-J. Lee, Phys. Rev. Lett. **125**, 207205 (2020).

[75] L. Leiva, S. Granville, Y. Zhang, S. Dushenko, E. Shigematsu, T. Shinjo, R. Ohshima, Y. Ando, and M. Shiraishi, Phys. Rev. B **103**, L041114 (2021).